

CFD Analysis on Aerodynamic Design Optimization of Wind Turbine Rotor Blades

R.S. Amano, R.J. Malloy

Abstract—Wind energy has been shown to be one of the most viable sources of renewable energy. With current technology, the low cost of wind energy is competitive with more conventional sources of energy such as coal. Most blades available for commercial grade wind turbines incorporate a straight span-wise profile and airfoil shaped cross sections. These blades are found to be very efficient at lower wind speeds in comparison to the potential energy that can be extracted. However as the oncoming wind speed increases the efficiency of the blades decreases as they approach a stall point. This paper explores the possibility of increasing the efficiency of the blades at higher wind speeds while maintaining efficiency at the lower wind speeds. The design intends to maintain efficiency at lower wind speeds by selecting the appropriate orientation and size of the airfoil cross sections based on a low oncoming wind speed and given constant rotation rate. The blades will be made more efficient at higher wind speeds by implementing a swept blade profile. Performance was investigated using the computational fluid dynamics (CFD).

Keywords—CFD, wind turbine blade, renewable energy.

I. INTRODUCTION

WIND turbine has been getting its attention as one of the most viable alternative power media. This paper explores two methods for optimizing blade for operation where wind speeds average 7m/s. The two methods of optimization that are investigated are first, the straight edge blade optimizes the angle of attack and chord length for a given airfoil cross section at different positions along the blade and second implements a swept blade profile. Among the factors outside the scope of the paper, technological advances in this field have allowed the price of wind energy to be competitive with more conventional sources. The blades are an important component of wind turbines and much research has been done in this area. Most commercial blades designs incorporate a straight edge span-wise profile with airfoil cross sections of various sizes and orientations. These designs have shown to be efficient in comparison to the amount of energy that can be extracted. The amount of energy in a column of wind seen by the swept area of a

turbine can be found from its kinetic energy and the power is expressed as follows [2]

$$P_{avail} = \frac{1}{2} \dot{m} V_0^2 = \frac{1}{2} \rho A V_0^3 \quad (1)$$

If momentum equation is solved across an idealized control volume about the turbine rotor it can be shown that the percentage of the total power available that can be extracted by a turbine is 16/27 or .59%. This limit is known as the Betz limit. Therefore the maximum power that a turbine can produce is expressed as follows

$$P_{max} = \left(\frac{16}{27}\right) \left(\frac{1}{2}\right) \rho V_0^3 A \quad (2)$$

Most turbines extract the maximum possible energy as defined above for lower wind speeds but gradually become less efficient as the on coming wind speed increases and the flow condition across the blades approach the stall condition. To illustrate this effect the power produced by a typical commercial turbine is compared to the amount of power available to it at various oncoming wind speeds in Fig 2. The turbine that is used is the Nordtank 500/41 with LM19.1 blades [1].



Fig. 1 NTK500/41 [1]

R.S. Amano is with the University of Wisconsin at Milwaukee, WI 53201 USA (corresponding author: 414-229-2345; fax: 414-229-6958; e-mail: amano@uwm.edu).

R.J. Malloy is a graduate research assistant at the University of Wisconsin at Milwaukee, WI 53201 USA (corresponding author: 414-229-2345; fax: 414-229-6958; e-mail: rjmalloy@uwm.edu).

As can be seen from Fig. 2 the power curve of the Nordtank NTK4500/41 wind turbine follows the maximum power curve up until about 10m/s oncoming wind speed. At this point the blades begin to stall and the turbine's performance levels off at around 600kW. This paper explores the possibility of

increasing the efficiency of the blades at higher wind speeds while maintaining efficiency at the lower wind speeds. The design intends to maintain efficiency at lower wind speeds by selecting the appropriate orientation and size of the airfoil cross sections based on a low oncoming wind speed and given constant rotation rate. The blades will be made more efficient at higher wind speeds by implementing a swept blade profile. The power generated from a blade using only the first optimization technique is compared to that generated from a blade using both techniques as well as that generated by NTK500/41 turbine using LM19.1 blades.

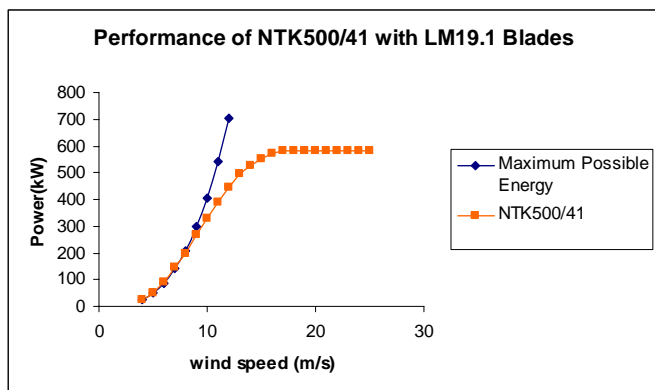


Fig. 2: Comparison of Available Wind Power and Power Output of NTK500/41 Turbine with LM19.1 Blades [2].

A. Straight Edge Blade

Wind turbine blades rely on lift produced by their airfoil cross sectional shapes to produce the torque at the base needed to turn the generator. Wind turbine blade profiles are often constructed using the Blade Element Momentum (BEM) theory. This theory produces the angle of twist and chord length for a given airfoil cross section and rotation speed at a finite number of positions along the span of the blade. From these two dimensional sections a three dimensional shape can be extruded. The BEM theory accomplishes this by treating a given cross section as an independent airfoil, which processes wind with a speed and direction that is a vector sum of the on coming wind speed and the wind speed generated by rotation (see Fig. 3 for the vectorial view).

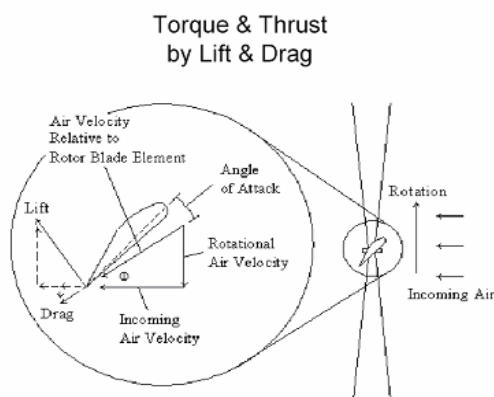


Fig. 3: Dynamics of a Wind Turbine Blade Cross Section [3]

Since the direction and magnitude of the wind generated by rotation changes as a function of span-wise position, the chord length and angle of attack of the airfoil cross sections must change as well.

The angle of twist is easily found at any position by adding the oncoming and rotational wind speed vectors. The chord length can be found by relating the thrust force to the lift force produced by a cross section. Thrust force is defined as the force experienced by the rotor in the stream-wise direction and is expressed as follows

$$T = \left(\frac{4}{9}\right) \rho V_0^2 A \quad (3)$$

The lift force is the force experienced perpendicular to the resultant wind vector with respect to airfoil and is expressed as follows.

$$L = \frac{1}{2} \rho V_a^2 A C_l \quad (4)$$

These two forces can be related as follows.

$$T = L \cos(\theta) \quad (5)$$

From equations 3 through 5 the following expression of chord length can be derived assuming a constant coefficient of lift value of 1 and neglecting drag. [2]

$$C = \frac{16\pi R \left(\frac{R}{r}\right) \cos(\theta)}{9\lambda^2 B} \quad (6)$$

The BEM approach does not correct for rotational motion. It is for this reason that CFD analysis is necessary for new blade designs. CFD does not use predetermined airfoil data to predict the blade performance. Instead it solves the governing fluid flow equations at thousands of positions on and around the blade in an iterative process. This approach allows the current airfoil model to take into account any span-wise wind velocity component which BEM theory cannot.

It was this method that was used to construct a straight edge blade prototype whose optimal on coming wind and rotation speeds were 7m/s and 20rpm, respectively. The blade has a length of 20m and uses the constant airfoil shape NACA 4412.

B. Swept Edge Blade

In addition to this straight blade, a swept edge blade was tested. This swept edge blade will have the same characteristics as the straight edge except for the trajectory of the edge. Each cross section will have the same dimensions and be at the same vertical distance from the hub as its corresponding section in the straight edge blade. The reason for testing this new geometry is that the straight edge blade is

constructed using a formulaic approach which treats the airflow over the blade as perfectly perpendicular to the leading edge and neglects any span-wise component. The swept edge blade profile aims to accommodate the span-wise velocity component and delay the stall point of the rotor. This geometry has largely been uninvestigated using the CFD approach. Recently an investigation into the loading and dynamic behavior of a swept blade was published by Larwood and Zureck [4]. They used codes developed by the National Renewable Energy Laboratories (NREL) which applied a more analytical approach. A CFD approach is more suitable for this investigation since it is purely an aerodynamic study and CFD yields very accurate results which are quantitative as well as qualitative.

II. NUMERICAL METHOD

A diffuser-shaped domain was chosen with a 120 degree slice taken lengthwise along the axis. Each side of the domain was given periodic boundary conditions. The front and top planes were given as velocity inlets. The rear plane was given as a pressure outlet. The domain extended 5 diameters upstream of the blade and 10 diameters downstream of the blade. The domain had a radial height of 5 diameters at the front and 8 diameters at the back. Several different mesh schemes were used in an effort to both resolve the boundary layer surrounding the blade and hub, and obtain a computationally feasible domain. A 4m×20m rectangle was constructed around the blade, and an unstructured mesh was used throughout the domain. Meshing proved to be a challenge due to the large differences in length scales in the domain. To achieve an adequate fine mesh that was still computationally feasible many size functions were utilized.

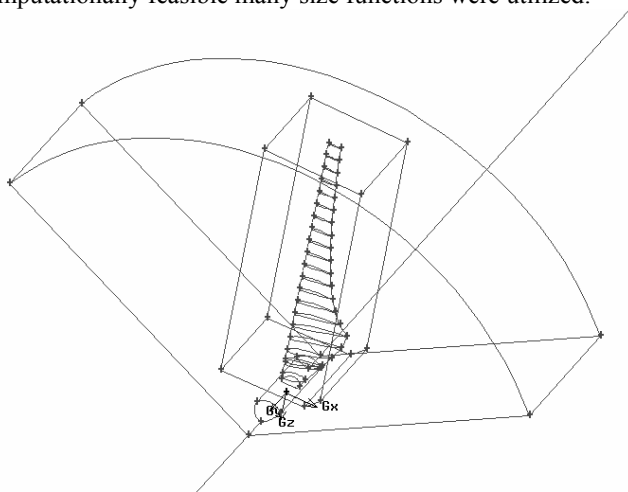


Fig. 4: Boundary Layer Resolution Approach

A start size of 0.007m was used at the leading and trailing edges of the blade along with a growth rate and maximum size of 1.14 and 0.05 extending onto the blade surfaces as shown in Fig. 4.

This approach adequately represented the aerodynamic shape of the blades. A starting size of 0.05 growth rate and

maximum size of 1.08 and 0.5 growth rates were attached to the blade surfaces and extended into the rectangular volume surrounding the blade. The wedge containing this rectangle and the rest of the blade/hub was meshed with a constant density mesh of 0.5m. The rest of the domain was given a growth rate of 1.08 and maximum size of growth rate 10 extending from this wedge.

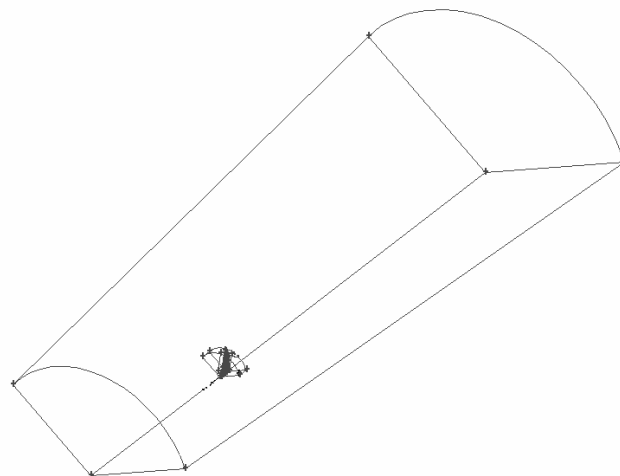


Fig. 5: Computational Domain

For the swept blade the rectangle was modified slightly to accommodate the swept edge geometry. This approach is based off of the work done by Mandas and Carcangiu [5]. The final mesh contained 1.7 million elements.

Seven different oncoming wind speeds were used ranging from 5m/s to 25m/s. This allowed for the construction of a power curve for each blade so they could be compared. The sides of the wedge were designated as rotational periodic boundaries. Finally the fluid being chosen as a moving reference frame was given a rotational speed of 2.09rad/s. The turbulence closure model used was the the κ - ω SST model. This model was used with success in a similar application by Ferrer and Munduante [6]. All results were obtained with a convergence criteria of the order of 10^{-5} . For validation of the results the same mesh scheme and domain were used to reproduce experimental data of NTK500 commercial wind turbine with LM19.1 blades. The results are shown below.

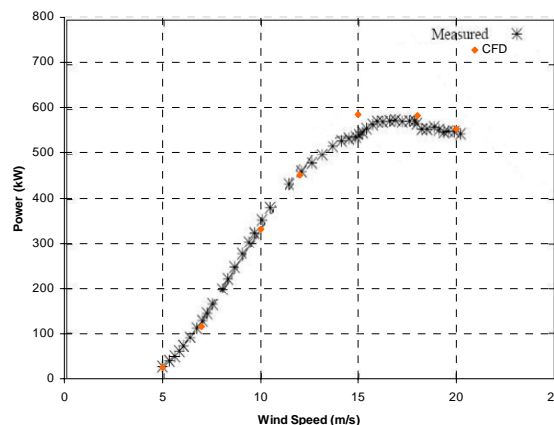


Fig. 6: CFD Predicted Performance of Commercial Wind Turbine NTK500 with LM19.1 Blades Compared to Experimental Data

As can be seen there is good agreement up until about 12m/s. Then the model brakes down as the blades begin to stall. The same effect was found by Mandas and C. Carcangiu [5]. This effect is not present with the two blades under investigation.

III. PRESENTATION OF RESULTS

Figures 7 and 8 show the pressure contours along the top upstream side of the straight and swept blades, respectively. It is clear from these two figures that the pressure level is higher on the swept blade, which confirms a higher lift force on the blade. This will enhance the power generated at the same upcoming stream velocity (wind speed).

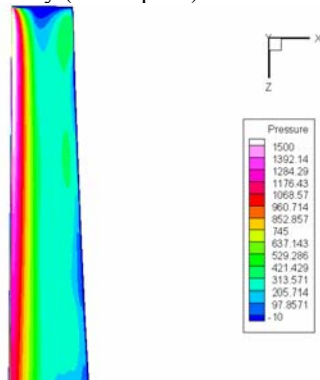


Fig. 7 Pressure Contours at the Top Upstream Side of the Straight Blade At 20m/s oncoming wind speed

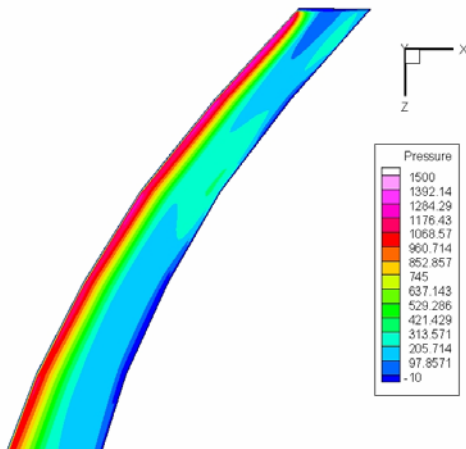


Fig. 8 Pressure Contours at the Top Upstream Side of the Swept Blade at 20m/s Oncoming Wind Speed

Figure 9 shows the predicted power curve of two turbines with the different blade geometries. From the figure it is clear that there is little performance variation at the lower oncoming wind speeds. This is desired because at these speeds the wind turbines are extracting the maximum amount of power as defined in equation 2. It can also be seen from Fig. 9 that the swept edge blade geometry produces an increase in power at higher wind speeds with the maximum being 15% occurring at 20m/s. It is clear that this increase is due to the swept edge geometry only since this was the only difference between the

blades besides a slight increase in frontal surface area as stated in Table 1.

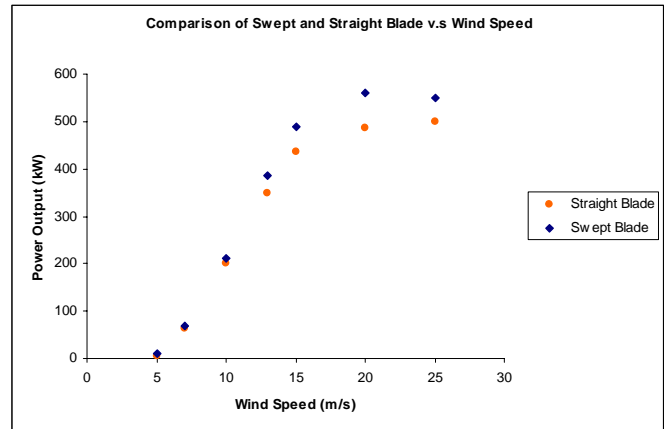


Fig. 9: CFD Predicted Performance of the Straight Edge and Swept edge Wind Turbine Blades

TABLE I SURFACE AREA COMPARISON

Edge Geometry	Surface Area(m ²)
Straight	89.3
Swept	90.77

From Figure 7 it should be noted that both geometries generate relatively the same amount of power as conventional large scale turbines such as NTK500/41 using LM 19.1 blades. The simulation for straight edge and swept edge blades also predicts stall effectively where as the simulation for the NTK500/41 turbine does not. Therefore the results shown in Fig 6 cannot completely verify the results shown in Fig 7. No experimental results of a turbine with the straight edge blade geometry, used in this investigation, are known to the author. Future work should incorporate experimental verification of results shown in Fig 7. A possible explanation for the difference in simulation performance is that the airfoil shape used in this investigation is slender compared to airfoil shapes used in typical blade design such as the NACA 63-418 used on the NTK500/41 turbine. Because of this shape characteristic the stall characteristics of the NACA 4412 airfoil are much more distinct and therefore can be modeled more easily. It is for this reason that this airfoil shape was chosen for this investigation.

IV. CONCLUSIONS

The following conclusions emerge from this study.

- (1) The simulation of the NTK500/41 satisfactorily validated the results of this investigation.
- (2) It was observed that the swept edge geometry maintains maximum efficiency at lower oncoming wind speeds and delays the stall point resulting in an increase in power at higher oncoming wind speeds.
- (3) The gain in the power is as high as 20 percent at higher speeds than 10m/s.

There are other methods that are used for optimizing blade performance that were not investigated here but should be

mentioned. One of the most obvious strategies is to increase the diameter of the rotor, because the swept area will contain more energy that can be abstracted. However this can be problematic as the loads at the hub/blade interface will increase dramatically. Research on relieving these loads through blade twist has been done by Larwood and Zuteck [4].

ACKNOWLEDGMENT

The authors are grateful to We Energies for their support on this project. The author is grateful to Mr. Carl Siegrist and Ms. Amy Flom for their great support to this research. Thanks are due to Mr. Jeremy Hogan for his dedicated assistance to the optimization study of wind turbine blades.

REFERENCES

- [1] NTK500/41
http://130.226.17.201/extra/web_docs/nordtank/WT_description.pdf
- [2] Hasen M. ,2000, "Aerodynamics of Wind Turbines"
- [3] Piggott H. "Small Wind Turbine Design Notes"
<http://users.aber.ac.uk/iri/WIND/TECH/WPcourse/index.html>
- [4] Larwood, S. and Zuteck, M., 2006, "Swept Wind Turbine Blade Aeroelastic Modeling for Loads and Dynamic Behavior".
- [5] Mandas, N., Cambuliand, F., and Carcangiu, C., 2006, "Numerical Prediction of Horizontal Axis Wind Turbine Flow," University of Cagliari, EWEC 2006, Athens, Business, Science, and Technology.
- [6] Ferrer, E. and Munduante, W., 2007,. "Wind Turbine Blade Tip Comparisons Using CFD." *Journal of Physics Conference series* 75, 012005

Ryo S. Amano (M'80—F'01). This author became a Member (M) of **ASME** in 1980 and a Fellow (F) in 2001.